Technical University of Denmark

DTU

Plasmonic anisotropic metasurfaces: from far-field measurements to near-field properties

Yermakov, Oleh Y.; Permyakov, Dmitry V.; Dmitriev, Pavel A.; Samusev, Anton K.; Iorsh, Ivan V.; Lavrinenko, Andrei; Bogdanov, Andrey; Zayats, Anatoly V.

DTU Library
Technical Information Center of Denmark

PROCEEDINGS OF SPIE

Plasmonic anisotropic metasurfaces: from far-field measurements to near-field properties

Oleh Y. Yermakov, Dmitry V. Permyakov, Pavel A. Dmitriev, Anton K. Samusev, Ivan V. Iorsh, et al.

SPIE.

Event: SPIE Photonics Europe, 2018, Strasbourg, France

Plasmonic anisotropic metasurfaces: from far-field measurements to near-field properties

Oleh Y. Yermakov[a], Dmitry V. Permyakov[a], Pavel A. Dmitriev[a], Anton K. Samusev[a],
Ivan V. Iorsh[a], Andrei V. Lavrinenko[b], and Andrey A. Bogdanov[a]

[a]Department of Nanophotonics and Metamaterials, ITMO University, St. Petersburg, Russia
[b]DTU Fotonik, Technical University of Denmark, Kongens Lyngby, Denmark

ABSTRACT

One of the most important problems of metamaterials and metasurfaces research is the derivation and the analysis of the effective parameters. They allow to examine the structure without singling out each element and it is the significant advantage for practical use. Recently, it has been shown that in virtue of a subwavelength thickness metasurfaces can be described within an effective conductivity approach. Such an effective surface conductivity describes the properties of a metasurface in the far-field as well as in the near-field. We derive and analyze the effective surface conductivity of a plasmonic resonant anisotropic metasurface theoretically and numerically. With the help of obtained effective conductivity we study the near-field properties of this metasurface, in particular, the equal frequency contours of surface waves. We show the topological transition from elliptical to hyperbolic-like dispersion regime for the surface waves on a hyperbolic metasurface. Finally, we study the influence of spatial dispersion on the eigenmodes spectrum and analyze the hyperbolic regime of a metasurface with strong spatial dispersion.

Keywords: hyperbolic metasurface, effective conductivity, effective parameters extraction, discrete dipole model, surface waves, spatial dispersion.

1. INTRODUCTION

The main feature of metamaterials is that electromagnetic properties of metamaterials can be homogenized, i.e. well described within an effective medium approximation. The key idea of this approach is to average microscopic fields and microscopic polarization satisfying microscopic Maxwell's equations and the continuity equation, which leads to the effective susceptibility, polarizability, permittivity, etc. This unique feature is possible due to the subwavelength period of the metamaterials structure and is not applicable for any other periodic structure such as photonic crystals.[1] Usually, for bulk metamaterials such effective parameters are the permittivity $\hat{\varepsilon}_{\text{eff}}$ and permeability $\hat{\mu}_{\text{eff}}$. Generally, these parameters are tensorial functions of frequency ω and wavevector $\mathbf{k}$.

Analogous homogenization procedures are relevant for metasurfaces – 2D analogues of metamaterials. Apparently, homogenization procedures for 2D structures were first developed in radiophysics and microwaves (equivalent surface impedance) in applications to thin films, high-impedance surfaces and wire grids etc.[2,3] It has recently been pointed out that two-dimensional structures, like graphene, silicene and metasurfaces, can be described within an effective conductivity approach.[4–8] In virtue of a subwavelength thickness, a metasurface could be considered as a two-dimensional equivalent current and, therefore, characterized by effective electric $\hat{\sigma}_e(\omega, \mathbf{k}_\tau)$ and magnetic $\hat{\sigma}_m(\omega, \mathbf{k}_\tau)$ surface conductivity tensors, where $\mathbf{k}_\tau$ is the component of the wavevector in the plane of the metasurface.[9,10] Importantly, such an effective conductivity allows to describe the interaction between a metasurface and propagating plane waves in the far-field (reflection, absorption, refraction, polarization transformation, etc.) as well as to forecast the spectrum of localized surface waves, i.e. to describe the interaction between a metasurface and evanescent waves in the near-field.

Further author information:
Send correspondence to Oleh Yermakov
E-mail: o.yermakov@metalab.ifmo.ru

The dispersion equation and set of equal frequency contours (EFCs) for the surface waves localized at anisotropic metasurface were analyzed in detail within effective conductivity approach in Refs. [6, 7]. It has been shown that the spectrum of an anisotropic metasurface consists of two eigenmodes with mixed TE-TM polarization, i.e. hybridization of the eigenmodes takes place.[6] It opens a route to the effective control over polarization and, as a consequence, spin angular momentum of surface waves.[11,12] The novelty of current work consists in studying the effect of nonlocal interaction on the eigenmodes dispersion. Particular attention is paid to the analysis and comparison of the hyperbolic regime in the framework of the effective medium approximation and in the presence of a nonlocal response (spatial dispersion).

2. MODEL AND METHODS

We consider an anisotropic metasurface placed in a homogeneous ambient medium with permittivity of fused silica ($\varepsilon = 2.1$). The target structure consists of 20 nm thick gold nanodisks with the elliptical base packed in the square lattice with a period of 200 nm. The long and short axes of the disks are $a_x = 134$ nm and $a_y = 103$ nm, respectively. The design of the sample is shown in Fig. 1.
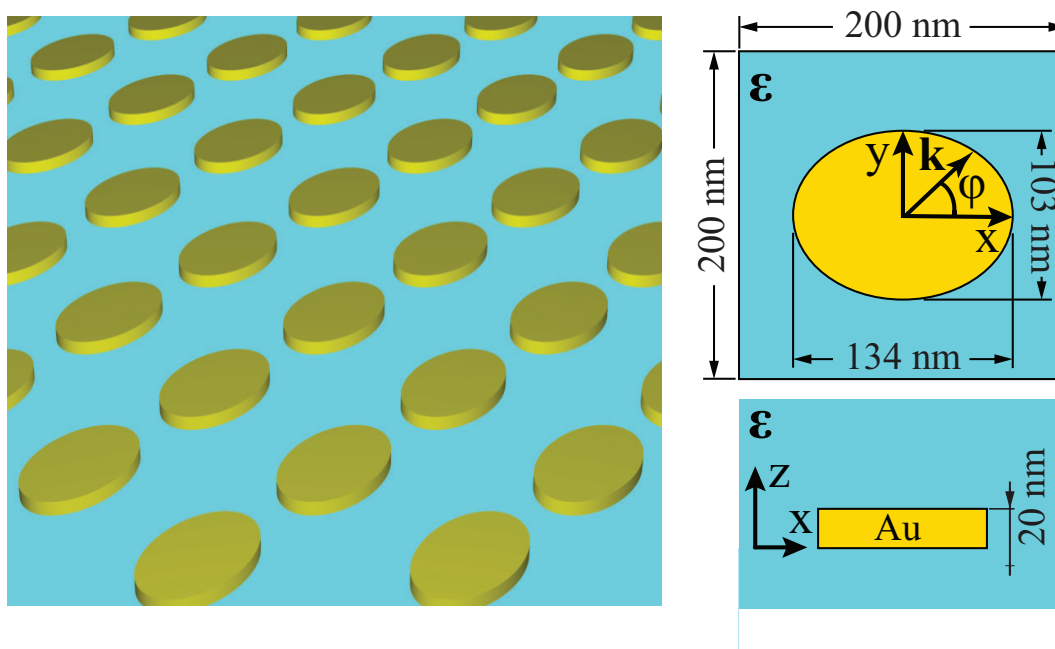

Figure 1. Anisotropic metasurface consists of 20-nm-thick gold nanodisks arranged in a square lattice (period 200 nm). The base of the disks has an elliptical shape, with the long and short axes equal to 134 and 103 nm, respectively. We assume the environment is uniform and isotropic with $\varepsilon = 2.1$.

On the one hand, we perform the extraction of effective conductivity tensor from the reflection spectra by applying the zero-thickness approximation developed in Refs. [13,14]. The reflection spectra can be simulated in CST Microwave Studio or measured experimentally.[13] After that we substitute the extracted conductivity into the dispersion equation derived in Refs. [6,11] and visualize the EFCs. In order to obtain the reflection spectra of the anisotropic metasurface coupled to a high-index ZnSe prism we use the transfer matrix method (TMM).[15]

On the other hand, we use the discrete dipole approximation (DDM), which takes into account the spatial dispersion effect.[16–19] Within this approximation we consider a periodic array of scatterers as an array of point dipoles, whereas polarizability of a separate scatterer coincides with the polarizability of the dipole, and calculate the interaction between the dipoles. This method is highly useful and applicable, because it easily allows to obtain the effective conductivity for other shapes of the particles without changing the lattice structure. In this case, we just need to recalculate one term – the polarizability of the single particle. The details and limitations of the discrete dipole model implementation are described in Refs. [13,20]. We verify theoretical results with the full-wave numerical simulation in COMSOL Multiphysics.

3. RESULTS AND DISCUSSION

It is convenient to present dispersion of surface waves in terms of equal frequency contours, which can be visualized in reflection experiments with a high index prism in Otto geometry.[21] We calculate reflection of a light wave in this configuration by using the transfer matrix method.[15, 22] When $\det[\mathrm{Im}(\hat{\sigma})] > 0$, the equal frequency contours have an elliptic shape (Figs. 2a, 2c, 2d, 2e). For a hyperbolic regime, when $\det[\mathrm{Im}(\hat{\sigma})] < 0$ ($\lambda = 730$ nm), the equal frequency contours represent a set of hyperbolas for the quasi-TE mode (Fig. 2b) and arcs for the quasi-TM mode (Fig. 2f). This drastic change of the shape is often called *topological transition*. One can see that in the hyperbolic regime both quasi-TE and quasi-TM modes are present, i.e. simultaneous propagation of two types of surface plasmons is observed (Figs. 2b and 2f). For the capacitive and inductive regimes only a single mode propagates. However, each mode has hybrid TE-TM polarization, so it is observed in both polarizations as shown in Fig. 2. Although polarization of the surface mode at 660 nm is predominantly similar to polarization of a conventional TM-plasmon (Fig. 2d), TE-polarization is also visible (Fig. 2a). The opposite situation takes place for a quasi-TE plasmon at $\lambda = 900$ nm (Figs. 2c and 2e). The exceptions are the principal axes directions where polarization of surface modes is strictly either purely TE or purely TM due to the lack of anisotropy.
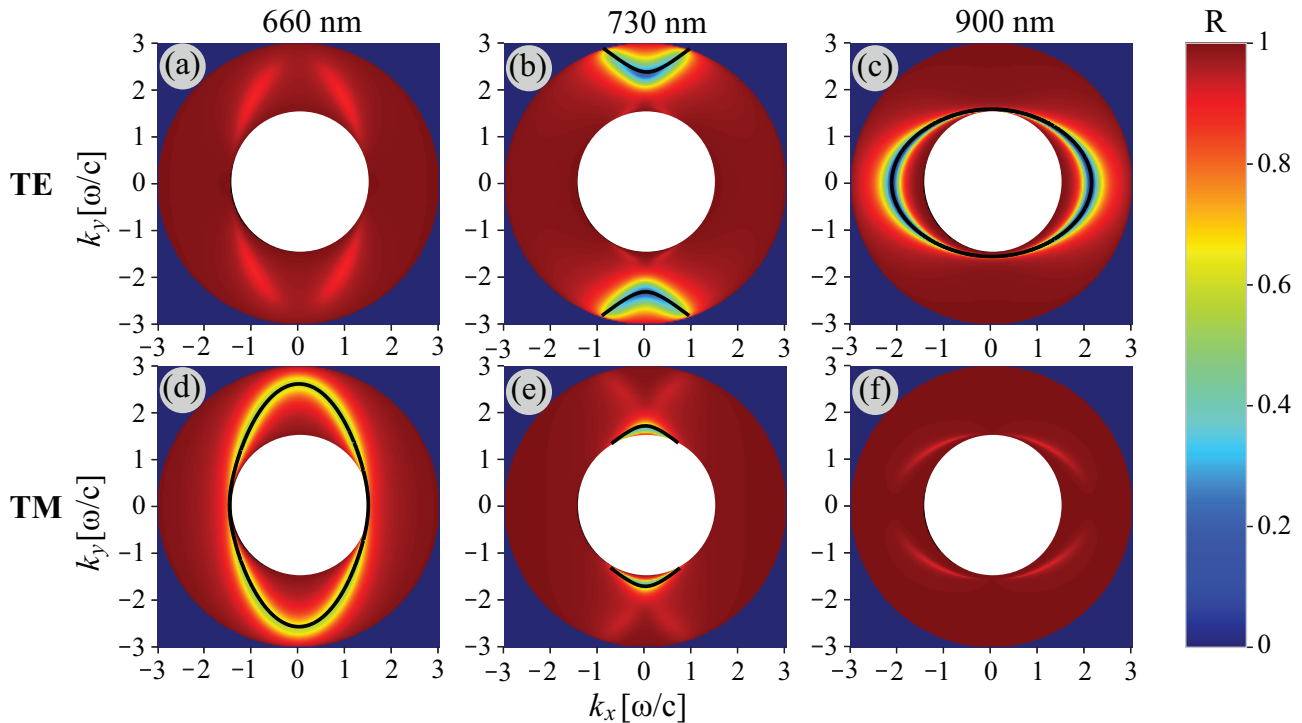

Figure 2. Simulation of the reflectance spectra with transfer matrix method from a metasurface shown in Fig. 1 for incident TE (a-c) and TM (d-e) polarizations. Panels (a) and (d), (b) and (e), (c) and (f) correspond to wavelengths $\lambda = 660, 730, 900$ nm, respectively. Black lines correspond to the equal frequency contours calculated from dispersion equation straightforwardly. White circle corresponds to the light cone in the embedded medium.

We compare the evolution and multiplicity of EFCs calculated (i) numerically and with discrete dipole model, i.e. taking into account spatial dispersion, and (ii) by using TMM and effective model for both TE (Fig. 3) and TM (Fig. 4) polarizations. Color maps in Figs. 3 and 4 correspond to numerical simulations carried out in COMSOL Multiphysics in top line and TMM calculations in bottom line. Black lines are the EFCs calculated within DDM in top line and by solving the dispersion equation using extracted effective conductivity in bottom line. It is important to note that we calculated EFCs within DDM at the wavelengths different from the simulated numerically ones. The axes in Figures 3 and 4 are normalized to ω/c units, curves borders in top line are limited by the first Brillouin zone.
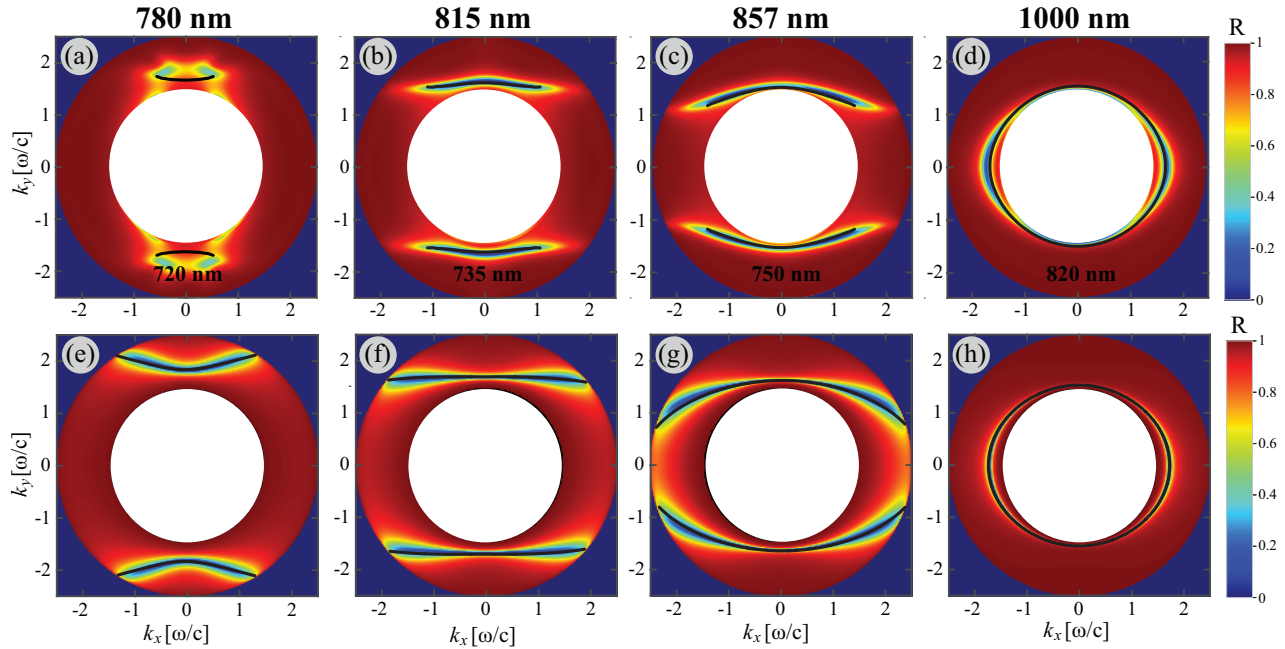
Figure 3. Comparison of the reflectance spectra from a metasurface shown in Fig. 1 for incident TE polarization calculated numerically (a-d) and by using TMM with effective conductivity (e-h). Panels (a) and (e), (b) and (f), (c) and (g), (d) and (h) correspond to wavelengths $\lambda = 780, 815, 857$ and 1000 nm, respectively. Black lines that correspond to the equal frequency contours are calculated by using DDM at different wavelengths in (a)-(d) and by solving dispersion equation from Ref. [6] straightforwardly in (e)-(h). White circles correspond to the light cone with $n = 1.45$, while big circles correspond to the light line in ZnSe with $n = 2.48$.
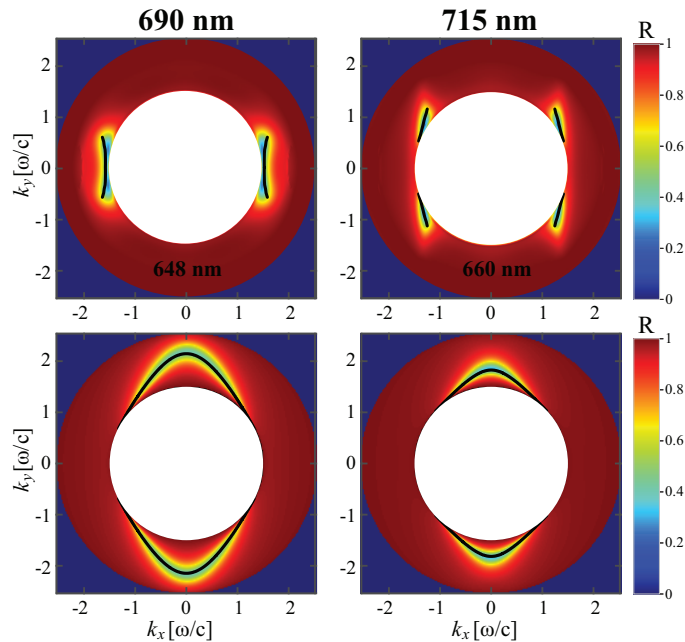

Figure 4. Comparison of the reflectance spectra from a metasurface shown in Fig. 1 for incident TM polarization calculated numerically (a,b) and by using TMM with effective conductivity (c,d). Panels (a) and (c), (b) and (d) correspond to wavelengths $\lambda = 690$ and 715 nm, respectively. Black lines that correspond to the equal frequency contours are calculated by using DDM at different wavelength in (a,b) and by solving from Ref. [6] straightforwardly in (c,d). White circles correspond to the light cone with $n = 1.45$, while big circles correspond to the light line in ZnSe with $n = 2.48$.

At low frequencies TE-like mode dispersion is close to the light line and both components of conductivity tensor are negative, which results into the ellipse at EFC (Figs. 3d and 3h). Between 857 and 1000 nm the EFC of TE-like mode becomes open, which leads to a forbidden range of propagation directions (Figs. 3c and 3g). However, for effective model it is still an ellipse for bigger values of wavevector components. At 815 nm the EFC is flat that conforms to the quasi one-dimensional propagation of TE-like surface mode (Figs. 3b and 3f). With the further decrease of the wavelength EFCs transform to the hyperbolas (Figs. 3a and 3e). Both effective model and DDM give qualitatively the same results for TE-like mode. The opposite situation takes place for TM-like mode, whereas numerical calculation and DDM strongly differ from the TMM and effective medium approximation (Fig. 4).

This comparison enables to study in detail the essence of a hyperbolic regime of a metasurface. In terms of the effective model, a hyperbolic regime corresponds to the indefinite anisotropic conductivity tensor and hyperbola-like EFCs.[23] The real picture is much richer and more complicated. Therefore, the question of hyperbolic regime of a metasurface with strong spatial dispersion effect remains open.

4. CONCLUSIONS

We have visualized the equal frequency contours of the surface waves localized at an anisotropic metasurface consisting of elliptical nanodisks in two ways: (i) by using effective medium approximation and (ii) by using discrete dipole model. Both models have been verified by transfer matrix method and full-wave numerical simulation. The effect of spatial dispersion was discussed, the topological transition from elliptical to hyperbolic-like dispersion regime was shown. Scientific and practical significance of the results highlights a number of potential applications in optical information technologies, opto-electronic and photonic devices, opto-mechanics, biological sensors, spin-controlled phenomena, etc.

ACKNOWLEDGMENTS

REFERENCES

[1] Zhukovsky, S. V., Andryieuski, A., Takayama, O., Shkondin, E., Malureanu, R., Jensen, F., and Lavrinenko, A. V., "Experimental demonstration of effective medium approximation breakdown in deeply subwavelength all-dielectric multilayers," *Phys. Rev. Lett.* **115**(17), 177402 (2015).

[2] MacFarlane, G., "Surface impedance of an infinite parallel-wire grid at oblique angles of incidence," *J. Inst. Electr. Eng. Part IIIA: Radiolocation* **93**(10), 1523–1527 (1946).

[3] Tretyakov, S. and Maslovski, S., "Thin absorbing structure for all incidence angles based on the use of a high-impedance surface," *Microw. Opt. Techn. Lett.* **38**(3), 175–178 (2003).

[4] Andryieuski, A. and Lavrinenko, A. V., "Graphene metamaterials based tunable terahertz absorber: effective surface conductivity approach," *Opt. Express* **21**(7), 9144–9155 (2013).

[5] Tabert, C. J. and Nicol, E. J., "Magneto-optical conductivity of silicene and other buckled honeycomb lattices," *Phys. Rev. B* **88**(8), 085434 (2013).

[6] Yermakov, O. Y., Ovcharenko, A. I., Song, M., Bogdanov, A. A., Iorsh, I. V., and Kivshar, Y. S., "Hybrid waves localized at hyperbolic metasurfaces," *Phys. Rev. B* **91**, 235423 (2015).

[7] Gomez-Diaz, J. S., Tymchenko, M., and Alù, A., "Hyperbolic plasmons and topological transitions over uniaxial metasurfaces," *Phys. Rev. Lett.* **114**(23), 233901 (2015).

[8] Nemilentsau, A., Low, T., and Hanson, G., "Anisotropic 2d materials for tunable hyperbolic plasmonics," *Phys. Rev. Lett.* **116**(6), 066804 (2016).

[9] Holloway, C. L., Kuester, E. F., Gordon, J. A., O'Hara, J., Booth, J., and Smith, D. R., "An overview of the theory and applications of metasurfaces: The two-dimensional equivalents of metamaterials," *IEEE Antenn. Propag. M.* **54**(2), 10–35 (2012).

[10] Glybovski, S. B., Tretyakov, S. A., Belov, P. A., Kivshar, Y. S., and Simovski, C. R., "Metasurfaces: From microwaves to visible," *Phys. Rep.* **634**, 1–72 (2016).

[11] Yermakov, O. Y., Ovcharenko, A. I., Bogdanov, A. A., Iorsh, I. V., Bliokh, K. Y., and Kivshar, Y. S., "Spin control of light with hyperbolic metasurfaces," *Phys. Rev. B* **94**, 075446 (Aug 2016).

[12] Yermakov, Y., Bogdanov, A. A., Iorsh, I. V., Bliokh, K. Y., and Kivshar, Y. S., "Tunable spin-directional coupling for surface localized waves with anisotropic metasurface," *Proc. SPIE* **10227**, 1022703 (2017).

[13] Yermakov, O. Y., Permyakov, D. V., Porubaev, F. V., Dmitriev, P. A., Baranov, D. A., Samusev, A. K., Iorsh, I. V., Malureanu, R., Bogdanov, A. A., and Lavrinenko, A. V., "Effective surface conductivity of plasmonic metasurfaces: from far-field characterization to surface wave analysis," *arXiv preprint arXiv:1712.07304* (2017).

[14] Yermakov, O., Mukhin, I., Samusev, A., Bogdanov, A., and Iorsh, I., "Effective conductivity tensor of plasmonic anisotropic metasurface: Theory and experiment," *P. Electromagn. Res. S.* , 1524–1528 (2017).

[15] Markos, P. and Soukoulis, C. M., [*Wave propagation: from electrons to photonic crystals and left-handed materials*], Princeton University Press (2008).

[16] Belov, P. A. and Simovski, C. R., "Homogenization of electromagnetic crystals formed by uniaxial resonant scatterers," *Phys. Rev. E* **72**(2), 026615 (2005).

[17] Poddubny, A. N., Belov, P. A., Ginzburg, P., Zayats, A. V., and Kivshar, Y. S., "Microscopic model of purcell enhancement in hyperbolic metamaterials," *Phys. Rev. B* **86**(3), 035148 (2012).

[18] Lunnemann, P. and Koenderink, A. F., "Dispersion of guided modes in two-dimensional split ring lattices," *Phys. Rev. B* **90**(24), 245416 (2014).

[19] Chebykin, A. V., Gorlach, M. A., and Belov, P. A., "Spatial-dispersion-induced birefringence in metamaterials with cubic symmetry," *Phys. Rev. B* **92**(4), 045127 (2015).

[20] Yermakov, O., Porubaev, F., Bogdanov, A., Samusev, A., and Iorsh, I., "Retrieval procedure of effective conductivity for plasmonic resonant anisotropic metasurface," *AIP Conf. Proc.* **1874**(1), 030040 (2017).

[21] Samusev, A., Mukhin, I., Malureanu, R., Takayama, O., Permyakov, D. V., Sinev, I. S., Baranov, D., Yermakov, O., Iorsh, I. V., Bogdanov, A. A., and Lavrinenko, A. V., "Polarization-resolved characterization of plasmon waves supported by an anisotropic metasurface," *Opt. Express* **25**(26), 32631–32639 (2017).

[22] Dmitriev, P., "kitchenknif/pyatmm: V1.0.0-a1." https://doi.org/10.5281/zenodo.1041040 (2017).

[23] Smith, D. and Schurig, D., "Electromagnetic wave propagation in media with indefinite permittivity and permeability tensors," *Phys. Rev. Lett.* **90**(7), 077405 (2003).